Available online at www.sciencedirect.com

ScienceDirect

Energy Procedia 62 (2014) 482 – 491

Energy Procedia

6th International Conference on Sustainability in Energy and Buildings, SEB-14

Control of Wind Conversion System Used in Autonomous System

Menad Dahmane*, Jérôme Bosche, Ahmed El-Hajjaji

Modélisation, Information & Systèmes Laboratory, 33 rue Saint Leu – 80039 Amiens, France

Abstract

The topology based on permanent magnet generator (PMSG) and diode bridge rectifier is frequently used in small wind energy conversion system since it is robust and easy to control. This paper presents a robust control for the wind conversion system based on PMSG and boost DC/DC converter in the aim to maintain the generator rectified voltage at a reference voltage corresponding to the reference power imposed by the supervisory module. The reference power control is guaranteed without measuring the wind speed. The sufficient conditions for state feedback stabilizing designed controller are given in terms of solutions to a linear matrix inequality (LMI) and H^{∞}. Simulation tests results are carried out for this wind conversion system topology which operates in a multi-source system, in order to visualize the feasibility of the proposed method.

Selection and peer-review under responsibility of KES International

Keywords: Wind conversion system, PMSG, Hybrid renewable system, LMI, Boost converter.

1. Introduction

Isolated power systems supplied with electricity by means of wind and other emerging forms of renewable energy are nowadays technically reliable options. These systems are often seen as more suitable for the local power supply in developing countries [6]. Indeed, it has been introduced essentially as green and reliable power systems for remote areas [9] [12]. This kind of systems strongly depends on the geographical and meteorological conditions of the installed region. Due to the intermittent nature of the wind and solar irradiation, the instantaneous power extracted from the wind turbine and PV panels sometimes does not match the instantaneous load demand. As a result, energy storage systems are essential for continuous and reliable operation. In addition, the energy storage devices provide transient stability during sudden load variations and they are very useful for load-leveling

* Corresponding author. Tel.: +33 651 523 251. *E-mail address:* menad.dahmane@u-picardie.fr.

Selection and peer-review under responsibility of KES International

doi:10.1016/j.egypro.2014.12.410

applications. There is a steady increase in usage of hybrid systems and consequently solving optimization problem for this system becomes necessity.

In this paper, we are only presented the wind conversion part from the hybrid system. The other parts are presented in [8-9]. Control of wind conversion system operating in hybrid system is required to track the power reference generated by the supervisory controller according meteorological conditions variations and changing in load demand [9] [11]. Specifically, there is many works in literature dealing with optimum power extraction from the wind conversion system by means of controlling rectifier converter or diode-bridge and boost/buck converter depending on the used topologies [3]. The wind conversion system topology used in this work consists of wind turbine based on permanent magnet synchronous generator (PMSG), diode rectifier, and boost converter which is connected to the dc bus. In wind conversion stage, permanent magnet synchronous generator is widely used especially for small installations. It provides various advantages over conventional generator such as gearless operation, higher efficiency, higher power density, higher power factor, larger power-to-weight ratio, and less maintenance [10].

The paper is organizes as the follow: In section two, a description of the global hybrid system is given, and moreover; a control strategy of the PMSG based wind conversion system is explained. In the third section; the simulation results of the robust control applied for this system is presented and we finish by conclusions and future work in section four.

Nomenclature

R	radius of the blades swept area
ρ	air density $\left(kg/m^3\right)$
β	pitch angle $\left(rad\right)$
ω_m	wind turbine rotational speed
C_p	turbine coefficient performance

2. Hybrid generation system

Stand-alone hybrid generation systems combine several generation modules, typically assimilating different renewable energy sources. In our project, we consider the wind-solar as the main energy sources. The objective of this system is to develop management algorithms in aims to provide without interruption, electrical energy of an isolate house. The architecture of concerned hybrid system is given by the figure bellow, it composed by wind system, solar system and storage system. In addition it consists of diesel engine as extra source fig.1.

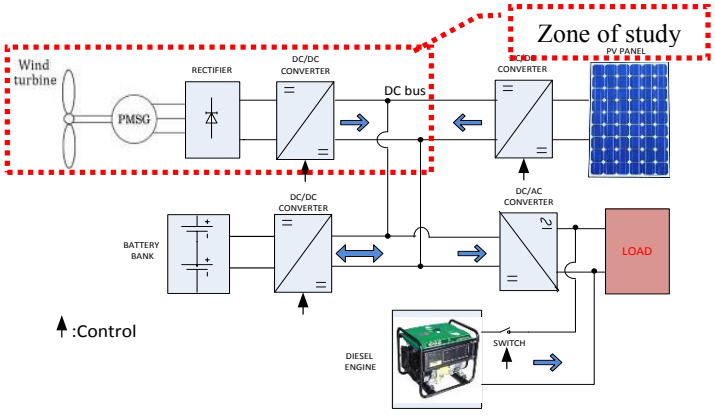

Fig. 1. Hybrid renewable energy conversion system.

However, the work treated in this paper is interested only in wind conversion subsystem.

2.1. Modeling of the wind conversion system

The wind conversion system used in this study consists of a small wind turbine coupled with permanent magnet synchronous generator of 1kW. The generator output voltage and frequency varies according to wind speed. These variables output of the generator are rectified using a diode bridge. The rectifier output feds a boost converter which allows changing the voltage of output of rectifier. The output of the boost converter is connected to the 100V DC bus, fig.2. Bulleted lists may be included and should look like this:

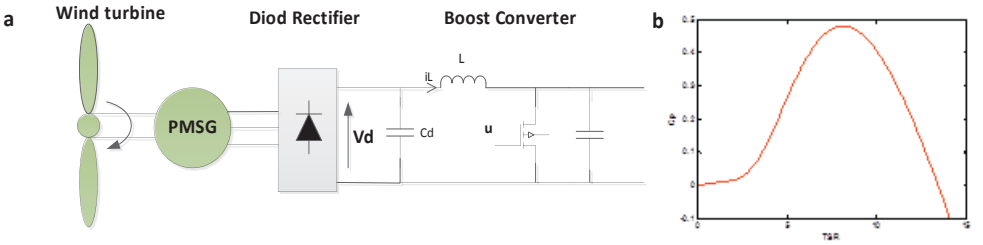

Fig. 2. (a) Wind conversion system based on PMSG ; (b) C_p curve used for in this paper

The power captured by the wind turbine (power delivered by rotor) is given by:

$$P_t = \frac{1}{2}.C_p(\lambda,\beta).\rho.A.V^3 = 0.5\rho AC_p \times \left(\frac{\omega_m R}{\lambda}\right)^3 \quad (1)$$

The tip-speed to wind speed ratio is given by $TSR = \lambda = \frac{\omega_m R}{V}$. Its curve variation is shown in fig.2b.

The models of the PMSG generator and the diode rectifier are developed using the SimPowerSystem® library of Matlab/Simulink®.

The DC/DC converter used in this study is boost converter type. The control of this converter can be achieved in order to control the wind power generated. In fact, track the power reference requires continuous variation of the dc voltage by means of the duty cycle of the boost converter fig.3.

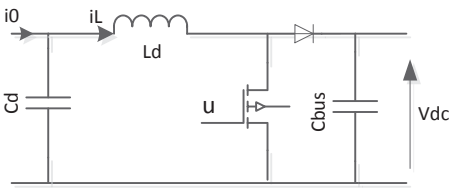

Fig.3. DC/DC boost converter

The average model of the electrical circuit is given by the following equations, such as v_D is the loss voltage in the diode and R_l is the resistance of the self-inductance.

$$\begin{cases} \frac{d}{dt} i_d = -\frac{R_l}{L_d} i_d + \frac{1}{L_d} V_d - \frac{(1-u)}{L_d}\left(V_{dc} + v_D\right) \\ \frac{d}{dt} V_d = \frac{-1}{C_d} i_d + \frac{1}{C_d} i_0 \end{cases} \quad (2)$$

Consider $x^T = \left[i_d, V_d\right] \in \mathbb{R}^{2x1}$ as the state vector where $A \in \mathbb{R}^{2X2}$ the state matrix, $B \in \mathbb{R}^{2X1}$ the input matrix, and, $W \in \mathbb{R}^{2X1}$ an exogenous input matrix. The stat representation is such that: $\dot{x} = Ax + Bu + W$

$$\begin{pmatrix}\dot{x}_1\\ \dot{x}_2\end{pmatrix}=\begin{pmatrix}\dfrac{-R_l}{L_d} & \dfrac{1}{L_d}\\ \dfrac{-1}{C_d} & 0\end{pmatrix}\begin{pmatrix}x_1\\ x_2\end{pmatrix}+\begin{pmatrix}\dfrac{V_{dc}+v_D}{L_d}\\ 0\end{pmatrix}u+\begin{pmatrix}-\dfrac{V_{dc}+v_D}{L_d}\\ \dfrac{i_0}{C_d}\end{pmatrix} \tag{3}$$

3. The proposed control strategy

The control strategy treated is this work is summarized in the following figure:

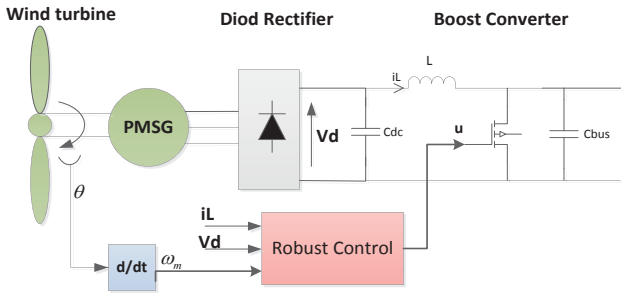

Fig. 4. Control strategy of the wind turbine

The DC/DC converter inserting between the rectifier output and the DC bus can change the DC voltage seen by the generator and therefore, the generator terminal voltage can be change. In other hand, the control of the wind turbine rotational speed allows changing the coefficient power, therefore, the electrical power generated by the wind turbine changed. Using relationship between turbine speed rotation and rectifier DC voltage; we can control the output power generated by the PMSG with applying adequate duty cycle of the boost converter. Furthermore, the converter is capable to increase or decrease the generator terminal voltage so is possible to capture wind energy in both high and low wind speed.

In the ideal steady-state; the relationship between terminal voltage and rotational speed can be obtained by considering a generator with a fundamental current in phase with terminal voltage and neglecting harmonic currents [5]. The torque equation can be obtained from (1):

$$T=\frac{P_t}{\omega_m}=\frac{1}{2\omega_m}.C_p\rho A\left(\frac{R\omega_m}{\lambda}\right)^3 \tag{4}$$

The generator-induced voltage and armature currents can be obtained from the manufacturer's data [5] by means of the governing torque and voltage equations.

$$\begin{cases}T=K_tI_a\\ E=K_e\omega_m\end{cases} \tag{5}$$

With T is the generator torque; I_a is the phase current; K_t and K_e are parameters given by the constructers. Indeed, consider the fact that the terminals of the generator are connected to a diode rectifier. It may be assumed that the phase voltage and fundamental component of the armature current of the generator are in phase. The phase voltage equation for a synchronous machine may be written as:

$$V=E-I_aj\omega_sL_s-I_aR_s \tag{6}$$

For unity power factor, we can write equation (6) as:

$$V=\sqrt{E^2-\left(I_a\omega_sL_s\right)^2}-I_aR_s \tag{7}$$

Where V is the terminal phase voltage R_s and L_s are the resistance and the self-inductance of the phase respectively; ω_s is the electrical angular speed and E is the electromotive force.

Since the output of the generator PMSG is connected to a three full bridge rectifier Fig. 2, the voltage at the rectifier output is written as follows:

$$V_d = \frac{3\sqrt{6}}{\pi} V - 2V_{diod} - \frac{3}{\sqrt{6}} \omega_s L_s I_a \tag{8}$$

With ω_s is the electrical angular frequency. Using the above relations, we can rewrite the voltage output of the rectifier as follows:

$$V_d = \frac{3\sqrt{6}}{\pi} \left(\omega_m \sqrt{K_e^2 - \left(\frac{TL_s p}{2K_t} \right)^2} - \frac{T}{K_t} R_s \right) - \frac{3}{\sqrt{6}} \frac{T}{2K_t} p \omega_m L_s \tag{9}$$

Where: $\omega_s = \frac{p}{2} \omega_m$; p is the number of poles and the diode loss voltage V_{diod} can be neglected and ω is the rotor speed.

We can see that this voltage is function of rotor speed and torque. So, for a given reference power $P_{ref} = T_{ref} \omega_m$, and by applying control of the dc-dc converter, speed and voltage varying continuously until they attaint their equilibrium. In this case the power reference is achieved. For this study, we supposed that the power reference is imposed by the power management algorithm. In this study, the power reference is imposed by the power management algorithm (supervision layer). Finally the output rectifier voltage is written as:

$$V_{d\_ref} = \frac{3\sqrt{6}}{\pi} \left(\omega_m \sqrt{K_e^2 - \left(\frac{T_{ref} L_s p}{2K_t} \right)^2} - \frac{T_{ref}}{K_t} R_s \right) - \frac{3}{\sqrt{6}} \frac{T_{ref}}{2K_t} p \omega_m L_s \tag{10}$$

Once the bus voltage reference is determined, we can calculate the duty cycle of the DC/DC converter (boost) that will follow this reference, and therefore, we follow the reference power given by the supervisory layer fig.5.

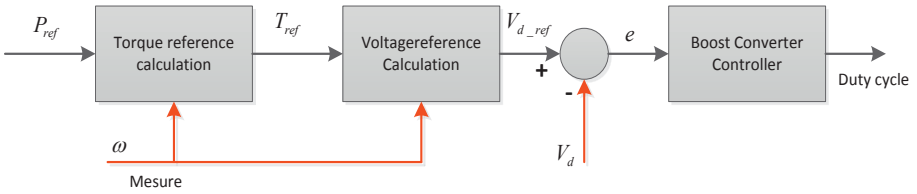

Fig. 4. Schematic diagram of the control strategy

In order to ensure a smooth tracking of the reference voltage, a new state variable is introduced. It corresponds to the integral of the tracking error ε as shown Fig. 6.

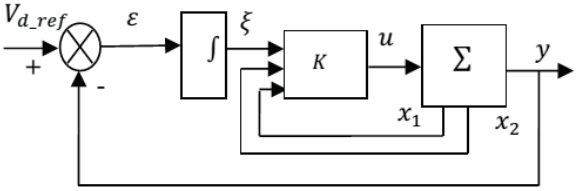

Fig.6. Closed-loop system architecture

We define $x_3 = \xi = \int \varepsilon$ with $\varepsilon = V_{d\_ref} - V_d = x_{2\_ref} - x_2$. The closed loop state space model is deducted from the two equations below:

$$\begin{cases} \dot{x} = Ax + Bu + D \\ \dot{x}_3 = \dot{\xi} = x_2 - x_{2\_ref} \end{cases} \tag{11}$$

The augmented model is written in this form:

$$\begin{pmatrix} \dot{x}_1 \\ \dot{x}_2 \\ \dot{x}_3 \end{pmatrix} = \begin{pmatrix} \frac{-R_l}{L_d} & \frac{1}{L_d} & 0 \\ \frac{-1}{C_d} & 0 & 0 \\ 0 & 1 & 0 \end{pmatrix} \begin{pmatrix} x_1 \\ x_2 \\ x_3 \end{pmatrix} + \begin{pmatrix} \frac{V_{dc} + v_D}{L_d} \\ 0 \\ 0 \end{pmatrix} u + \begin{pmatrix} -\frac{1}{L_d} & 0 & 0 \\ 0 & \frac{1}{C_d} & 0 \\ 0 & 0 & 1 \end{pmatrix} \begin{pmatrix} V_{dc} + v_D \\ \frac{i_0}{C_d} \\ V_{d\_ref} \end{pmatrix} \tag{12}$$

4. TS fuzzy Model

Since the DC link voltage is not really fixe, because it varies around a fixed value, it can be considered as a non-linearity witch can be bounded between two fixed values: $V_{dc} = \left[\underline{V_{dc}}, \overline{V_{dc}}\right]$

Furthermore, we can extract the Takagi-Sugeno model (TS) corresponding. This one is a polytope in two peaks, will greatly simplify the problem of feasibility of LMIs. So we obtain:

$$\overline{B}_1 = \begin{pmatrix} \frac{\underline{V_{dc}} + v_D}{L_d} \\ 0 \\ 0 \end{pmatrix}; \quad \overline{B}_2 = \begin{pmatrix} \frac{\overline{V_{dc}} + v_D}{L_d} \\ 0 \\ 0 \end{pmatrix} \tag{13}$$

The T-S fuzzy model describes nonlinear system by combining local linear dynamic subsystems in ***IF − THEN*** fuzzy rules. By taking $z = V_{dc}$ as a non-linearity; the previous model (12) can be represented by the following T-S fuzzy rules:

Rule(i): $IF\ z(t)\ is\ F_i\ THEN\ \dot{X} = \overline{A}X + \overline{B}_i u + B_w \overline{W}$ (14)

With $i = 1, 2.$ is the number of rules. By using the singleton fuzzifier; the product fuzzy inference and weighted average defuzzifer, the inferred output of the fuzzy system is:

$$\dot{X} = \sum_{i=1}^{2} h_i\left(z(t)\right)\left(\overline{A}X + \overline{B}_i u + B_w \overline{W}\right) \tag{15}$$

5. State feedback Control with H-infinity performance

5.1. Synthesis of controller with LMI technics

The control signal is obtained using parallel distributed compensation (PDC) and this control is written as:

$$u = -\sum_{i=1}^{2} h_i\left(z(t)\right) K_i X \tag{16}$$

With: K is state feedback gain and X is the augmented state vector. The closed loop model is then written as:

$$\dot{X} = \sum_{i=1}^{2}\sum_{j=1}^{2} h_i h_j\left(z(t)\right)\left(\overline{A} - \overline{B}_i K_j\right) X + B_w \overline{W} \tag{17}$$

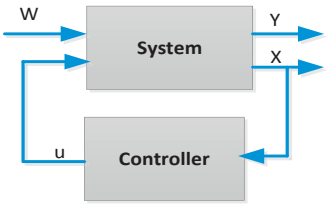

Fig. 7 Block diagram of state feedback control

- LMI formulation for H-infinity performance: Given the closed loop system (12), we denote the influence of $\overline{W}$ on the tracking error ε by the Root Mean Square (RMS) gain (H-infinity norm) as:

$$\|T\| = \sup_{\|W\|_2 \neq 0} \frac{\|\xi\|_2}{\|W\|_2} \tag{18}$$

Theorem1. Given the system (13), the *H-infinity norm* T does not exceed γ if and only if there exists a quadratic Lyapunov function: $V(\mathrm{X}) = X^T PX$ with $P = P^T > 0$ such as:

$$\frac{dV(\mathrm{X})}{dt} + \xi^T \xi - \gamma^2 \bar{W}^T \bar{W} < 0 \tag{19}$$

With $\xi = \int \left(V_d - V_{d\_ref} \right) = \int \varepsilon$.

The development of the condition (15) allows writing [7]:

$\frac{dV(X)}{dt} = \dot{X}^T PX + X^T P\dot{X}$ becomes after development:

$$\dot{V}(X) = \begin{pmatrix} X^T \\ \bar{W}^T \end{pmatrix} \begin{pmatrix} \left(A - B_i K_i\right)^T P + P\left(A - B_i K_i\right) & PB_w \\ B_w^T P & 0 \end{pmatrix} \begin{pmatrix} X \\ \bar{W} \end{pmatrix} < 0$$

To check this inequality, it suffices to check that:

$$\begin{pmatrix} \left(A - B_i K_i\right)^T P + P\left(A - B_i K_i\right) & PB_w \\ B_w^T P & 0 \end{pmatrix} < 0 \tag{20}$$

The development of the $\xi^T \xi - \gamma^2 \bar{W}^T \bar{W}$ allows writing:

Being: $\xi^T \xi - \gamma^2 \bar{W}^T \bar{W} = \left(C_e X\right)^T C_e X - \gamma^2 \bar{W}^T \bar{W} < 0$; with $C_e = \begin{bmatrix} 0 & 0 & 1 \end{bmatrix}$.

In other form $\xi^T \xi - \gamma^2 \bar{W}^T \bar{W} = \begin{pmatrix} X^T \\ \bar{W}^T \end{pmatrix} \begin{pmatrix} C_e^T C_e & 0 \\ 0 & -\gamma^2 I_1 \end{pmatrix} \begin{pmatrix} X \\ \bar{W} \end{pmatrix} < 0$

To check this inequality, it suffices to check that:

$$\begin{pmatrix} C_e^T C_e & 0 \\ 0 & -\gamma^2 I_1 \end{pmatrix} < 0 \tag{21}$$

The combination of both expressions (20) and (21) gives the following *BMI* (Bilinear Matrix Inequality):

$$\begin{pmatrix} \left(A - B_i K_i\right)^T P + P\left(A - B_i K_i\right) + C_e^T C_e & PB_w \\ B_w^T P & -\gamma^2 I_3 \end{pmatrix} < 0 \tag{22}$$

After linearization of this BMI and using the Schur lemma, we obtain the following LMI:

$$\begin{pmatrix} \Phi_i & QC_e^T & B_w Q \\ C_e Q & -I_1 & 0 \\ QB_w^T & 0 & -\gamma^2 I_3 \end{pmatrix} < 0 \tag{23}$$

Where $\Phi_{ij} = QA^T + AQ - Y_j{}^T B_i^T - B_i Y_j$; $Q = P^{-1}$ and $Y_j = K_j P$

- LMI formulation for Poles placement

The objective is to design a controller such that the closed-loop eigenvalues are placed in sub region in the complex left half plane to achieve desired behaviours [14]. Specifically, this is to place the poles of the augmented system in a region of the left half complex plane to ensure a certain level of transient performance. The poles placement considered in this paper is the $\alpha - stability$ [13] [14]. The characteristic function in LMI region is given is by:

$$D = \left\{ y \in \mathbb{C} \mid f_D(z) = \alpha + \beta y + \beta^T \bar{y}^T < 0 \right\} \quad (24)$$

Where $\alpha \in \mathbb{R}^{l*l}$ and $\beta \in \mathbb{R}^{l*l}$ are matrix defining the structure of LMI region.

Therefore the following LMI can be deduced in the case of $\alpha - stability$ using theorem given in [14] with $\alpha = 2a$ and $\beta = 0$

$$2aP + \left(A - B_i K_i\right) P + P\left(A - B_i K_i\right)^T < 0 \quad (25)$$

With a a parameter defined the remoteness of the LMI region of the imaginary axis.

Conclusion: the controller gains are calculated by solving LMIs (23) and (25).

6. Simulation results

The simulation of the wind conversion system is carried out using Matlab/Simulink® as shown in Fig.8. The numerical illustration considers the wind conversion system with the parameter values given by the Table.

After calculation of the voltage reference, a robust control based on LMI technics is designed to good following this reference. The simulation results to illustrate this are given bellow.

Table 1. Wind conversion system data

Effective Turbine Radius	1.2 m
Phase to phase winding Inductance	3.3 mH
Phase to phase winding Resistance	5.8 Ω
Peak per phase Torque Constant	0.71 Nm/A
Poles	8
System inertia	0.0012 kg/m^2
System dumping	0.016 Nm/kRPM

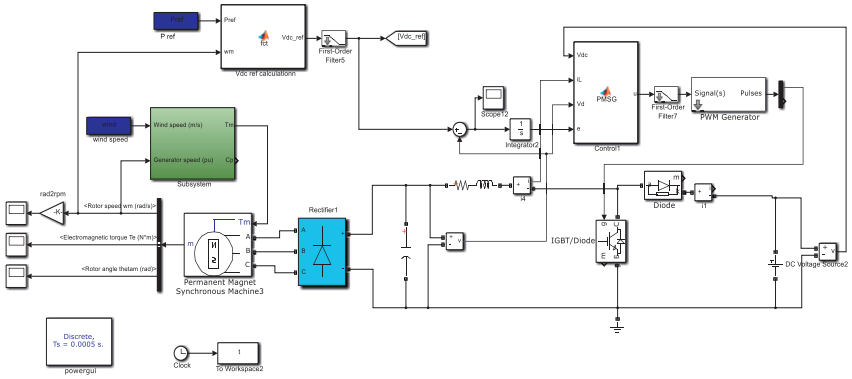

Fig.8. Block diagram of state feedback control

The parameters used in this simulation are taken in the literature witch correspond to a 1.5kW PMSG generator [5].

The simulation result is given by the following. In the fig.9, we tested our control response using an echelon in wind speed at t=5s.

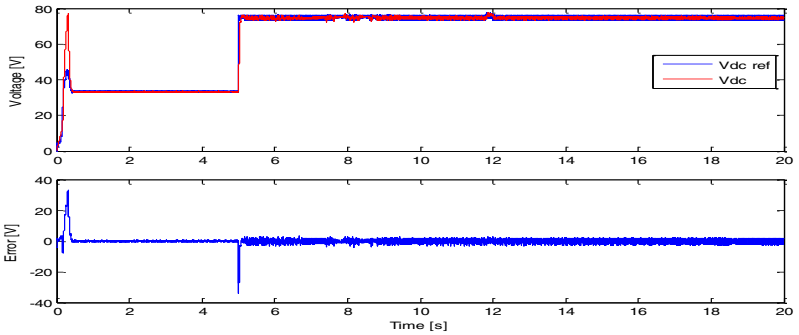

Fig.9. Vdc reference tracking

In another case, we simulate the system using reel wind speed profile as fig.10 which corresponds to the day of March, 11th 2013 in Amiens region France.

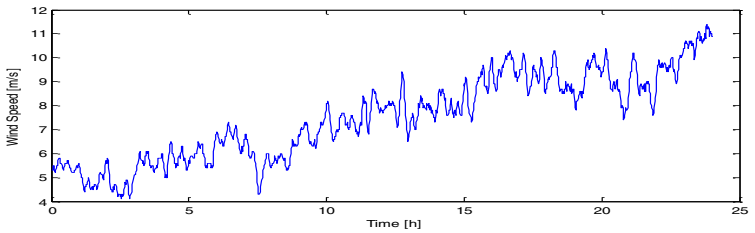

Fig.10. Real profile of wind speed

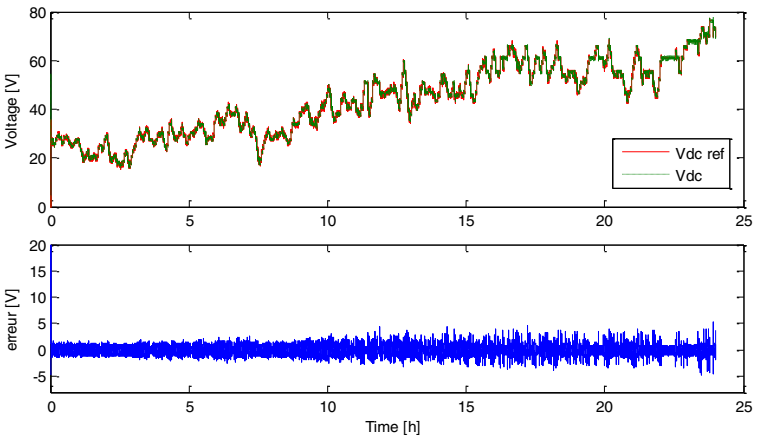

Fig.11. Vdc reference tracking

Observation:

These figures show the effectiveness of the control applied to the boost converter. Fig.10 illustrates the response of the control against instantaneous variation of the voltage reference, we can see the quality of the reference tracking in the fig 9. In the second case (fig.11), we illustrate the control behavior according a real profile of the wind speed and we can see the good tracking of the reference which is justified by the he figure of error tracking.

7. Conclusion

In this paper, a control of wind conversion system operate in stand-alone multi-sources system is presented. The treated problem in this work deals with tracking reference power of a PMSG wind conversion system by calculation of the dc voltage reference of the rectifier output which corresponds to the reference power. By using robust control based on LMI techniques of the boost converter, allowed to track this voltage reference; and therefore track the power reference. In order to ensure a good transient performances and quick response, the controller gains are designed with poles placement in LMI region. Numerical simulations using real measurement of wind speed has validated the proposed control strategy.

As future work, we project to test this control in our test bench and thereafter connect all sources as presented in fig.1 in order to implement management strategies.

References

1] S. Boyd, L.E. Ghaoui, V. Balakrishnan, Linear Matrix Inequalities in System and Control Theory, SIAM, Philadelphia, PA, 1994.

[2] A. Urtasun, P. Sanchis, I. San Martín, J. López, L. Marroyo. Modeling of small wind turbines based on PMSG with diode bridge for sensorless maximum power tracking. Renewable Energy, 2013, 55: 138-149.

[3] N. A. Orlando, M. Liserre, V. G. Monopoli, R. A. Mastromauro, A. Dell'Aquila. Comparison of power converter topologies for permanent magnet small wind turbine system. IEEE International Symposium on Industrial Electronics (ISIE). 2008,p, 2359 – 2364.

[4] M. E. Haque, M. Negnevitsky, K. M. Muttaqi .A Novel Control Strategy for a Variable Speed Wind Turbine with a Permanent Magnet Synchronous Generator. IEEE Transaction on Industry Applications, Vol. 46, No. 1. 2010, p. 331-339.

[5] A. M. Knight, G. E. Peters. Simple Wind Energy Controller for an Expanded Operating Range. IEEE Transactions on Energy Conversion, Vol. 20, No. 2, 2005, p.459-466.

[6] M. Lopez. Contribution a l'Optimisation d'un Systeme de Conversion Eolien pour une Unite de Production Isolée. PhD thesis, Université Paris Sud.

[7] S-K Hong, R. Langari. An LMI-based H^{∞} fuzzy control system design with TS framework. Information Sciences 123. 2000, p. 163-179.

[8] M. Dahmane, J. Bosche, A. El Hajjaji, X. Pierre. MPPT for photovoltaic conversion systems using genetic algorithm and robust control. American Control Conference (ACC), 2013, p. 6595 – 6600.

[9] M. Dahmane, J. Bosche, A. El Hajjaji. Renewable Energy Management Algorithm for Stand–alone System. International Conference on Renewable Energy Research and Applications (ICRERA). Madrid 2013.

[10] M. N. Uddin, M. M. I. Chy. A Novel Fuzzy-Logic-Controller-Based Torque and Flux Controls of IPM Synchronous Motor. IEEE Transactions on Control Systems Technology. Vol.46, No.3, Jan. 2010.

[11] W. Qi, J. Liu, X. Chen, and P. D. Christofides. Supervisory Predictive Control of Standalone Wind/Solar Energy Generation Systems. IEEE Transactions on Control Systems Technology. Vol.19, No.1, Jan. 2011.

[12] M. Dali, J. Belhadj, X. Roboam. Hybrid solarewind system with battery storage operating in grid–connected and standalone mode: Control and energy managementeExperimental investigation. Energy. Vol.35. 2587-2595.

[13] J. Bosche. Analyse et commande par placement de poles en DU-stabilité robuste. Ph.D. Thesis Université de Poitiers. 2003.

[14] M. Chilali and P. Gahinet. $H\infty$ Design with Pole Placement Constraints: An LMI Approach. IEEE Transactions on Automatic Control, vol. 41 (3) pp. 358–367, 1996.